Substrate Induced Thermal Decomposition of Perfluoro-Pentacene Thin Films on the Coinage Metals

ARTICLE *in* THE JOURNAL OF PHYSICAL CHEMISTRY C · SEPTEMBER 2012

Impact Factor: 4.77 · DOI: 10.1021/jp307316r

5 AUTHORS, INCLUDING:

Tobias Breuer
Philipps University of Marburg
21 PUBLICATIONS **134** CITATIONS
SEE PROFILE

Stefan Wippermann
Max Planck Institute for Iron Research GmbH
37 PUBLICATIONS **364** CITATIONS
SEE PROFILE

Gregor Witte
Philipps University of Marburg
38 PUBLICATIONS **931** CITATIONS
SEE PROFILE

THE JOURNAL OF PHYSICAL CHEMISTRY C

Article

pubs.acs.org/JPCC

Substrate Induced Thermal Decomposition of Perfluoro-Pentacene Thin Films on the Coinage Metals

Christian Schmidt,[†] Tobias Breuer,[†] Stefan Wippermann,[‡] Wolf Gero Schmidt,[§] and Gregor Witte*[,†]

[†]Molekulare Festkörperphysik, Philipps-Universität Marburg, D-35032 Marburg, Germany

[‡]Department of Chemistry, University of California, One Shields Avenue, Davis, California 95616, United States

[§]Lehrstuhl für Theoretische Physik, Universität Paderborn, D-33095 Paderborn, Germany

ABSTRACT: The thermal and chemical stability of perfluoropentacene (PFP) thin films grown by organic molecular beam deposition onto the (111)-oriented surfaces of the coinage metals copper, silver, and gold have been studied by means of temperature dependent X-ray photoelectron spectroscopy (XPS) and Near-Edge X-ray absorption fine structure spectroscopy (NEXAFS). Under vacuum conditions, PFP multilayers are completely desorbed at 425 K while molecules in contact with the Au(111) surface remain intact up to 500 K. By contrast, PFP that is in contact with Cu(111) is distinctly distorted and becomes partially defluorinated already upon thermal desorption of multilayers. A pronounced defluorination of PFP also takes place on Ag(111) at temperatures around 440 K, while further heating causes a complete cracking and defluorination. Additional measurements carried out on a regularly stepped silver surface demonstrate that steps are active sites that promote defluorination already at lower temperatures. van der Waals corrected density-functional (DFT-D) calculations show that PFP, though being weakly adsorbed on all three metal surfaces, exhibits a reduced energy barrier for defluorination, in particular on copper and silver, thus reflecting their catalytic activity. The calculations reveal further that defluorinated molecules are covalently bound to the substrate, leading to a notable bending of the molecular backbone. The present study highlights the importance of also considering chemical reactions when theoretically analyzing molecule/metal interactions and indicates that fluorinated aromatic molecules, though offering interesting electronic properties, actually exhibit a limited stability in contact with some electrode surfaces like silver due to catalytic effects.

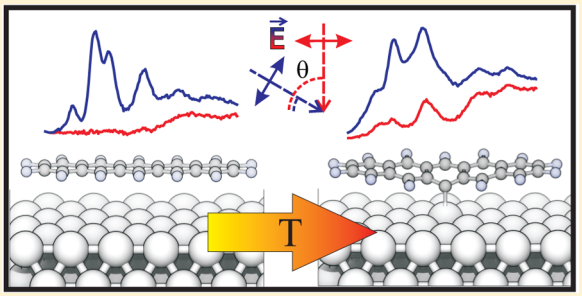

INTRODUCTION

The promising potential of organic electronic applications has triggered considerable research activities aiming at the synthesis of new organic semiconductor (OSC) materials with improved properties.[1,2] In addition to enhanced charge carrier mobility, also improved chemical stability is an important issue since most OSCs exhibit a low threshold for oxidation, leading to a notable degradation under ambient conditions.[3−5] One strategy to avoid such parasitic reactions is based on fluorination of the organic compound, which not only suppresses oxidation but also makes OSC films more hydrophobic, such that additional capping might be redundant.[6] Recently, this approach was also applied to larger acenes such as pentacene (PEN) by the synthesis of perfluoro-pentacene[7] (PFP, Figure 1a). It was further shown that perfluorination also affects the charge carrier polarity, rendering PFP an interesting n-type OSC.

Another aspect of key importance for the successful realization of organic electronic devices is the interaction between OSCs and metals, since it determines the resulting injection barrier of charge carriers at electrodes. Regarding the interaction between PFP and the (111) surfaces of the coinage metals Cu, Ag, and Au, the work function change and adsorption geometry have been studied by means of UPS and XSW.[8−10] In all cases, the vertical adsorption distance between the aromatic plane and the metal surface was found to be about 0.5 Å larger than for the nonfluorinated PEN, while the work function reduction is distinctly smaller than for PEN. These findings have also been obtained in a recent density functional theory study and were attributed to a pronounced Pauli repulsion due to the high electron density of the fluorine atoms.[11] Because of the supposed stability of PFP, only little attention has yet been paid to the thermal and chemical stability of PFP layers adsorbed on metals. Interestingly though, evidence for partial decomposition of PFP on Cu(111) above room temperature was reported,[9,12] while PEN monolayers adsorbed on the more reactive Cu(110) surface can be heated up to 600 K without any noticeable degradation.[13] Similarly surprising was our recent finding that thermal induced decomposition of PFP on Ag(111) occurs already below 450 K.[14] This suggests that on Ag(111) PFP is actually *less* stable than the nonfluorinated analogue which was found to desorb *intactly* at 550 K from Ag(111).[15] Even more surprising is the behavior found for smaller fluoroacenes such as perfluorobenzene. In that case, a decomposition of molecular adlayers is

Received: July 24, 2012
Revised: September 12, 2012

   dx.doi.org/10.1021/jp307316r | *J. Phys. Chem. C* XXXX, XXX, XXX−XXX

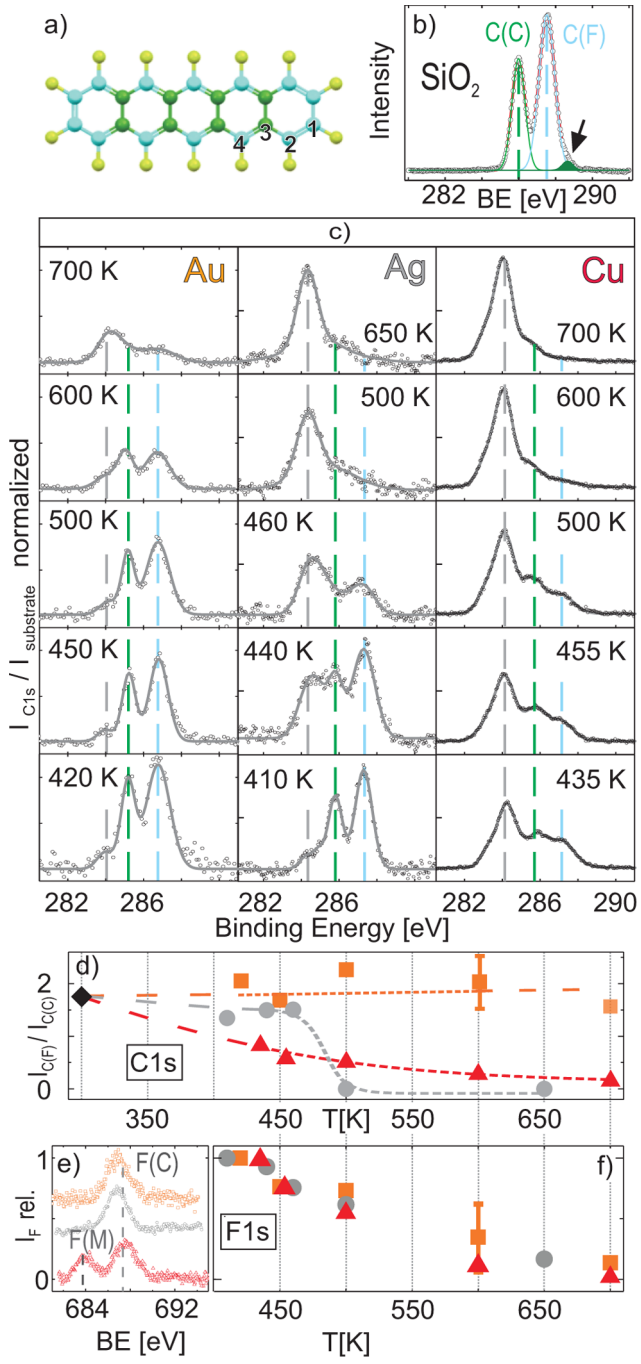

Figure 1. Summary of XPS data obtained for PFP films. Panel b displays the C1s region of a 70 nm PFP film on SiO_2 exhibiting two carbon species, C(C) and C(F), according to their chemical coordination within the molecule as depicted in part a and an additional shake up signal (black arrow, see text). Panel c displays the thermal evolution of XP spectra of PFP monolayer films on the three metal surfaces (Au, orange; Ag, gray; Cu, red) together with (d) the ratio of the carbon species C(F) and C(C). F1s spectra shown in part e revealed only one species on gold and silver, F(C), while on copper also the second species F(M) was found. The thermal evolution of the F(C) intensities is shown in part f.

reported upon heating on polycrystalline silver substrates,[16] while an intact desorption is found for Cu(111).[17] This is counterintuitive, since copper is the more reactive metal, which demonstrates a lack of understanding of the chemical interaction of fluoroacenes and metal surfaces.

As these findings challenge the general concept of fluorinated OSCs, we believe a systematical study to be very important. Therefore, we have studied the thermal stability of PFP adsorbed on the coinage metal surfaces Cu(111), Ag(111), and Au(111) by means of temperature dependent high resolution synchrotron based X-ray photoelectron spectroscopy (XPS) and X-ray absorption spectroscopy (NEXAFS). Particular attention was paid to possible radiation damages as well as to the influence of defects like surface steps. The latter was achieved by additionally examining the stability of PFP films on a vicinal silver Ag(221) surface. To understand the underlying mechanism of the observed decomposition, we performed total-energy calculations based on density-functional theory (DFT). By calculating a potential energy surface for chemical reactions, possible reaction pathways for the decomposition as well as belonging energy barriers were derived.

METHODOLOGY

Experimental Section. All measurements were carried out at the HE-SGM dipole beamline at the synchrotron storage ring facility BESSY II in Berlin (Germany). The X-ray photoemission spectra were recorded at an incident angle of 45° and at normal emission using a hemispherical electron energy analyzer (Scienta R3000) using typical pass energies of 100 eV and photon energies between 500 and 880 eV depending on the substrate and the studied region (C1s or F1s) chosen such that parasitic contributions by, e.g., auger lines were omitted. To provide a precise energy calibration, the XPS binding energies have been referenced to characteristic substrate peaks of the various samples (Au $4f_{7/2}$ 84.0 eV, Ag $3d_{5/2}$ 368.1 eV, Cu $3p_{3/2}$ 75.0 eV)[18] which have been measured simultaneously. The spectra have been corrected by subtracting a Shirley background[19] and dividing by the intensity of the corresponding substrate signals to compensate variations of the photon flux. After that, spectra have been normalized to the maximum intensity of each series to enable comparison. Carbon edge NEXAFS spectra were recorded by measuring the secondary electron yield as a function of photon energy of the linearly polarized (polarization factor 91%) incident synchrotron light. The exit slit of the grating monochromator was chosen such that an energy resolution of about 300 meV was achieved. To enhance surface sensitivity of NEXAFS by essentially detecting auger electrons from surface-near layers and reducing secondary electrons emitted from deeper layers and the surface, a retarding field of −150 eV was applied to the entrance grid of the channel plate detector (*partial electron yield at fixed detector position*).[20] To calibrate the absolute energy scale of the NEXAFS spectra, a simultaneously recorded signal of the photocurrent from a carbon coated gold grid in the incident beam was used which exhibits a sharp resonance at 284.9 eV. All NEXAFS raw data have been normalized with respect to the incident photon flux, and the transmission characteristics of the clean substrates were considered. Different types of metal substrates have been examined in the present experiments. While a Cu(111) and a Ag(221) single crystal were used, the Au(111) and Ag(111) samples consist of 150 nm metal films epitaxially grown on freshly cleaved mica substrates under UHV conditions. All samples were prepared in situ by repeated sputtering and annealing procedures, providing sharp LEED patterns and carbon free XP spectra. All perfluoropentacene (PFP, Kanto Denka Kogyo, purity >99%) films were deposited onto the various substrates at room temperature from a Knudsen cell at a typical growth rate of 10 Å/min, which

dx.doi.org/10.1021/jp307316r | J. Phys. Chem. C XXXX, XXX, XXX−XXX

was monitored by quartz microbalance. To suppress disturbing signatures from multilayer films and to prepare a nominal monolayer, at first 10 nm of PFP were deposited and subsequently excess multilayers were thermally desorbed by carefully heating the samples to about 410−430 K. Note that this procedure results in a *nominal monolayer*, which does not necessarily equal a *densely packed* layer.[21]

COMPUTATIONAL

The total-energy calculations are performed using the Vienna Ab Initio Simulation Package (VASP)[22] and employing the PW91 functional[23] for the generalized gradient approximation to the electron exchange and correlation (XC) energy. The electron−ion interaction is described by the projector-augmented wave method,[24] which allows for a relatively moderate energy cutoff of 400 eV for the plane-wave basis. The adsystem was modeled by periodically repeated supercells, containing six atomic coinage metal layers arranged in a (7×4) translational symmetry, the adsorbed molecules, and a vacuum region of 15 Å. The calculations were performed using the equilibrium lattice constants that we determined to be 3.63, 4.17, and 4.19 Å for Cu, Ag, and Au, respectively. Brillouin zone integrations are restricted to the Γ point. The smearing of the electronic states is performed with the Methfessel−Paxton scheme of the first order with a width of 0.2 eV.

The accurate modeling of loosely bonded adsorbates is a major challenge for density-functional theory (DFT), because the currently used XC energy functionals do not properly describe the long-range vdW interactions.[25−30] In order to account approximately for dispersion interactions, we use a semiempirical, so-called DFT-D scheme[31,32] based on the London dispersion formula. Reuter and co-workers[28] compared adsorption energies calculated within various DFT-D schemes for the adsorption of benzene on coinage metal (111) surfaces with experimental data and concluded that the approach by Ortmann et al.[31,32]—the one which is used in the following—provides results in the *"right ballpark and could even be semiquantitative"*. Similar conclusions can be drawn from benchmark calculations by Blügel's group[27] for a variety of small, π-conjugated molecules adsorbed on Ag(110). In these calculations, the approximate treatment of dispersion interactions with DFT-D was compared with a more realistic vdW density-functional (vdW-DF) approach.[33] It turned out that—depending on the molecule—the calculated total adsorption energies differ by 50−200 meV. Relative energy differences calculated within either scheme agree within 30−120 meV. It should be borne in mind, however, that vdW-DF is an approximation as well; see, e.g., the results in refs 30 and 34. Altogether, one has to state that the accurate description of dispersion forces for complex systems is not satisfactorily solved yet.[29] Still, since we are primarily interested in energy differences calculated for identical molecules with similar adsorption geometries on different coinage metal (111) surfaces, the present DFT-D scheme is expected to be sufficiently accurate to allow for valid conclusions.

RESULTS

XPS. The thermal stability of PFP monolayer films adsorbed on (111) surfaces of the three coinage metals gold, silver, and copper was at first characterized by means of temperature dependent XPS measurements. This offers a quantitative analysis of the film composition and thus enables monitoring of desorption and chemical alteration processes. To begin with, XP spectra were recorded for a 70 nm PFP film deposited onto SiO_2 to provide bulk-like reference spectra of PFP without any chemical substrate interaction, which are virtually identical to those obtained for multilayer films on gold. As shown in Figure 1b, the C1s signal is split into two peaks according to the different chemical environment of carbon atoms within the molecules.[9,35] The signal at a binding energy of 286.0 eV corresponds to the inner-ring carbon, only bound to neighboring carbon atoms, C(C), while the second, more intense peak at 287.5 eV is due to carbon atoms bound to fluorine, C(F). We note that the two subcomponents exhibit a different peak width (C(C), 0.71 eV; C(F), 0.86 eV), which can be related to slight variations of the chemical shift of C(F) atoms according to different fluorine coordination of their next nearest carbon atoms. As depicted in Figure 1a, this leads to the presence of four different carbon species, [C(C), C(F) surrounded by two C(C), C(F) surrounded by C(C) and C(F), and C(F) surrounded by two C(F)] with a multiplicity ratio of (8:6:4:4). Since the different C(F) species could not be separated in the present data, they were merged and treated as one effective C(F) peak for the analysis of the stoichiometry. The quantitative analysis of the C(C) and C(F) peak areas yields a ratio of 4:7 as expected for PFP. In addition, a rather weak but distinct shoulder appears in the C1s region at a binding energy of 289.2 eV (indicated by the black arrow in Figure 1b), which is attributed to a shakeup satellite. Since it remains unclear whether this signal originates from the C(F) or C(C) peak, the corresponding energy loss amounts to 1.1 or 2.7 eV, respectively. Note that these energies differ from the lowest excitation at 1.75 eV found in optical absorption spectra of PFP films.[36,37] A similar situation has been reported by Rocco et al.[38] for nonfluorinated acenes where the energy loss of shakeup satellites is smaller than the optical HOMO−LUMO band gaps, which might be attributed to the different band gap of the final ionic state formed in the photoemission process.

To examine the thermal stability of PFP monolayer films on the different coinage metals, the samples were in each case heated with a rate of approximately 1 K s^{-1} to the denoted temperature before the belonging XP spectra were acquired during cooldown. Figure 1c compares the thermal evolution of the C1s signal. The C1s signals of PFP monolayers on Ag(111) and Au(111) resemble the bulk data, except from a core-hole screening shift due to the underlying metal of about −0.7 eV.[14,35] By contrast, the PFP monolayer on Cu(111) prepared by briefly heating the sample to 435 K exhibits a new, dominating carbon signal around 284 eV (indicated by a dashed gray line). The binding energy of this new peak, which was also observed in a recent study by Glowatzki et al. for heated PFP films adsorbed on Cu(111),[12] indicates the presence of a nonfluorinated carbon species, while the broad peak width hampers a clear distinction between aliphatic or aromatic species which are energetically rather similar. A similar species appears on the Ag(111) surface after heating the PFP adlayer to 440 K where it becomes dominating at 460 K and above. We note that hydrocarbonaceous contributions were observed earlier for PFP films on metals and had been attributed to contaminations or decomposition reactions at surface defects.[9,35] For a quantitative analysis of the temperature dependent XPS measurements, the background-subtracted and normalized areas of the C(C) and C(F) peaks are determined. Figure 1d compares the thermal evolution of the

dx.doi.org/10.1021/jp307316r | J. Phys. Chem. C XXXX, XXX, XXX−XXX

intensity ratios C(F)/C(C) of nominal PFP monolayers on the various metal substrates. The black diamond at 300 K represents the ratio found for the undisturbed bulk reference film (cf. Figure 1b). At temperatures between 400 and 460 K, the C(F)/C(C) signal ratio obtained for PFP films on silver and gold well corresponds to the stoichiometry of PFP within the experimental error. By contrast, the PFP molecules on copper exhibit a distinct reduction of the fluorinated carbon species and the $I_{C(F)}/I_{C(C)}$ ratio decays continuously with increasing temperature. Above 460 K, also the progression of the $I_{C(F)}/I_{C(C)}$ ratio on the noble metals differs. As indicated in our previous study,[14] where a laboratory X-ray source was used, massive decomposition of PFP molecules on Ag(111) occurs already slightly above the multilayer desorption temperature. (This refers to the temperature at which multilayers have desorbed during *our heating protocol*. We note that the process is thermally activated and occurs in a nonequilibrium situation under UHV conditions so that a real *desorption temperature* is not precisely defined.) By contrast, the $I_{C(F)}/I_{C(C)}$ ratio does not significantly change for a PFP monolayer on gold upon heating, though the total carbon intensity decreases which suggests a partial desorption of intact molecules. Only after annealing at 700 K, a small carbonaceous signal of non-fluorinated species arises, which might be attributed to molecular decomposition occurring at defects or to contaminations diffusing from the sample holder. Note that, due to the low intensity caused by thermal desorption, the ratio given in Figure 1d for the last data point is poorly defined. The temperature dependent XPS measurements thus indicate a decomposition of PFP on Cu and Ag, while intact desorption dominates on Au.

In addition, F1s spectra were recorded after every heating step. The quantitative analysis of the peak intensity yields a continuous decrease with increasing temperature for all metals, as shown in Figure 1f. Typical F1s spectra of heated PFP monolayers (450 K) on Au(111) and Ag(111) are shown in Figure 1e, which exhibit only one fluorine species, F(C), as expected from the molecular structure. By contrast, on Cu(111), an additional fluorine species arises upon heating (best visible in the 600 K spectrum shown in Figure 1e), which we assign to copperfluoride, F(M).[18]

NEXAFS. In a next step, temperature dependent carbon edge X-ray absorption measurements were carried out, which allow for determination of the position of unoccupied molecular electronic levels. This information enables a chemical distinction between aromatic and aliphatic units and can be used to complement the XPS data in order to understand the different thermal stability of PFP on the various metals. Moreover, the dichroism of the NEXAFS signatures yields additional information about the orientational ordering of the adsorbed molecules.[20] The top panel of Figure 2 shows a typical normalized C1s NEXAFS spectrum of a PFP multilayer film on SiO_2 that was recorded at an incident angle of $\theta = 55°$ of the field vector $\vec{E}$ relative to the surface normal. On the basis of our previous analysis,[21] the first four peaks (285.3, 286.2, 286.8, and 288.3 eV) can be assigned to excitations of C1s electrons into unoccupied π^* orbitals, while the other resonances appear at energies larger than the continuum step (indicated in the NEXAFS spectrum at 450 K on Au(111) in Figure 2b) and therefore can be attributed to σ^* resonances or Rydberg states. The sharp π^* resonances also appear for PFP monolayers on Au(111) and Ag(111) in the spectra taken at grazing incidence (θ = 30°, blue curves). This indicates the

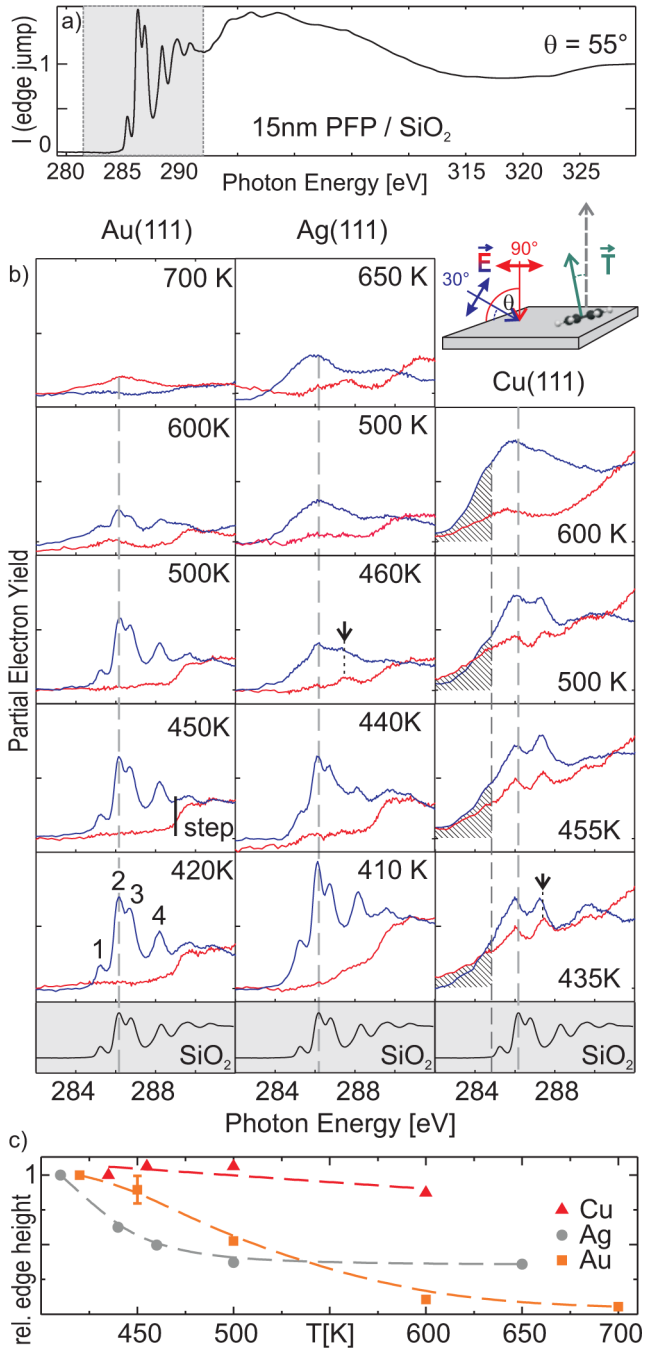

Figure 2. Series of carbon edge NEXAFS spectra of PFP films: (a) full spectrum of a 15 nm thick multilayer on SiO_2 that is used as a reference, together with (b) enlarged spectra of the π^*-region for PFP monolayers on the three metal surfaces recorded after applying different heating steps. For comparison, the relaxation-shift corrected π^*-region of the reference spectrum (a) is also shown in the bottom row. The experimental geometry illustrating the color code and the transition dipole moment of vector type π^* orbitals are depicted in the upper right. Panel c shows the thermal evolution of the height of the carbon edge jump relative to that after the first heating step (i.e., nominal monolayer).

absence of any distinct modification of unoccupied molecular orbitals of PFP due to chemical interaction with the underlying noble metal and suggests an almost van der Waals (vdW) type interaction. For PFP, only a small relaxational shift of about 0.2 eV occurs between NEXAFS data of multi- and monolayer

dx.doi.org/10.1021/jp307316r | J. Phys. Chem. C XXXX, XXX, XXX−XXX

films, due to the underlying metal substrate.[39] NEXAFS spectra of a PFP monolayer on the noble metals taken at normal incidence ($\theta = 90°$, red curves) reveal no π^* resonances, hence showing a pronounced dichroism which reflects a flat lying adsorption geometry (for a quantitative analysis, see Marks et al.[21]). Figure 2 shows further a series of magnified C1s NEXAFS spectra of the π^* region of PFP monolayer films adsorbed on the three metals as a function of the annealing temperature. For each heating step, the NEXAFS spectra were recorded subsequent to the respective XPS measurements. To also provide information about the molecular orientation, the NEXAFS data were taken at normal and grazing incidence. Analyzing the peak area of the individual resonances provides a comparison of the remaining contribution of a species. Moreover, the height of the carbon edge jump (i.e., difference of intensities at 330 and 270 eV) allows for a quantitative monitoring of the overall carbon coverage (see Figure 2c), which corroborates the trend obtained in the temperature dependent XPS measurements (cf. Figure 1d,f).

In contrast to the noble metal substrates, the PFP monolayer on Cu(111) exhibits a distinctly different NEXAFS signature already after thermal desorption of the excessive multilayer (i.e., the first heating step). Instead of four sharp resonances, only one broad resonance around 286 eV remained visible, while the others are smeared out, yielding a broad background signal. In addition, a new peak appears in the NEXAFS spectra at 287.3 eV (indicated by a black arrow), as well as noticeable intensity at energies lower than the first peak of the PFP bulk spectra (hatched area). Since the latter signals appear only for π^* resonances of nonfluorinated carbon species, they indicate the formation of fluorine-free fragments with C−C double bonds which might coke upon further heating. Moreover, the distinct NEXAFS signatures were not only observed at grazing incidence (blue curves) but also seen at normal incidence (red curves), which reveals a changed dichroism. Though this might indicate a change in the molecular orientation, it should also be taken into consideration that the molecular orbitals can be distorted due to chemical interaction with the substrate, such that the transition dipole moment, $\vec{T}$, of the π^* transitions is no longer perpendicular to the aromatic ring plane.[40,41] Therefore, a quantitative analysis of the tilt angle can be misleading[42] and was omitted. A similar situation occurs for pentacene monolayers chemisorbed on Cu(110) where a noticeable dichroism was found in the NEXAFS data[13] although the adsorbed molecules are not tilted.[43] Using standing X-ray waves, it has been demonstrated that PFP molecules adsorbed on Cu(111) also exhibit a distinct geometrical distortion leading to an upright bending of the fluorine atoms.[9]

Upon further annealing, quite different changes appear in the NEXAFS spectra. On Au(111), the distinct signature of the four sharp π^* resonances as well as the pronounced dichroism remain clearly visible up to temperatures of more than 500 K, while the intensity of these resonances and hence the coverage are reduced upon heating above 450 K. This reflects a thermal desorption of entire molecules without noticeable decomposition, which is in agreement with the findings of the temperature dependent XPS measurements (cf. Figure 1). Only for temperatures above 600 K, an additional, broad peak with a reduced dichroism appears around 286 eV, which might be attributed to a thermally induced fragmentation and coking. In view of the rather high temperature of this process, where virtually all molecules are desorbed from the Au(111) surface, the remaining signal is attributed to a minority of molecules that were more firmly bound to defects. In contrast to gold, the thermal evolution of PFP films on Ag(111) is quite different. In the case of the silver sample already after heating to 440 K, a noticeable broadening and intensity reduction of the π^* resonances can be recognized. Briefly heating the film only 20 K higher causes a complete disappearance of the fine structure and the appearance of a new peak at 287.3 eV (indicated by the arrow), as found already in the first annealing step on Cu(111). Further heating causes an additional peak broadening, while the NEXAFS spectra still reveal a distinct signal, even when heating to 650 K. The overall carbon coverage decreases, but in contrast to the case of Au(111), firmly bound species are found up to high temperatures for Ag(111). The thermal evolution of NEXAFS spectra of PFP on Cu(111) very much resembles the situation found for Ag(111) at elevated temperatures. Already after the first heating step, the distinct fine structure has disappeared and only a broad π^* resonance around 286 eV is visible besides the new peak at 287.3 eV. Both features remain visible upon heating up to 500 K and perish in a broad but intense NEXAFS signal, which extends also to lower energies than the first resonance of the PFP bulk spectrum (hatched area) after heating to 600 K. Interestingly, the new spectral feature at 287.3 eV always appears when the nonfluorinated C1s signal (at 284 eV) occurs and simultaneously the C(C) peak (at 286 eV) is still visible in XPS. As shown in Figure 2c, the total carbon coverage remains nearly constant on Cu(111), thus indicating that nearly all molecules are firmly bound after defluorination occurring already during heating at 435 K and do not thermally desorb upon further heating.

Defects. The presented XPS and NEXAFS data clearly demonstrate that the stability of PFP monolayer films depends significantly on the supporting metal substrate. As surface defects such as steps are known to strongly influence catalytic reactions,[44] complementary measurements were carried out for a vicinal silver surface. This material was chosen, as the reactivity of silver was found to be in between that of gold and copper. In particular, a Ag(221) surface was chosen (cf. Figure 3d), as it provides a high density of well-defined monatomic steps. Their lateral separation of 8.7 Å is slightly larger than the molecular width and thus may allow for an aligned adsorption of PFP on the (111) terraces like it was found for PEN on Cu(221).[45] The corresponding NEXAFS spectra of a PFP monolayer that had been prepared by heating a multilayer film to 410 K are displayed in Figure 3a. Like in the case of copper, the π^* resonances found in the bulk spectrum are strongly attenuated and broadened, while a distinct new resonance at about 287.3 eV appears, which developed on the Ag(111) surface only after heating to 460 K. Moreover, in contrast to the PFP film on Ag(111), the dichroism is clearly reduced and the spectral features were also observed at normal incidence (red curve). To discriminate whether this intensity is primarily due to thermal decomposition or due to the different surface geometry of the silver surfaces,[46] additional measurements were carried out for a submonolayer film of PFP by depositing a nominal thickness of less than 2 Å without heating prior to data acquisition. As shown in Figure 3b, the NEXAFS spectra of this preparation again yield four distinct sharp π^* resonances with a pronounced dichroism like on the inert Au(111) surface. This clearly demonstrates that the distinct spectral changes found for the PFP monolayer film on Ag(221) prepared by thermal desorption of excessive multilayers are caused by a thermally

dx.doi.org/10.1021/jp307316r | J. Phys. Chem. C XXXX, XXX, XXX−XXX

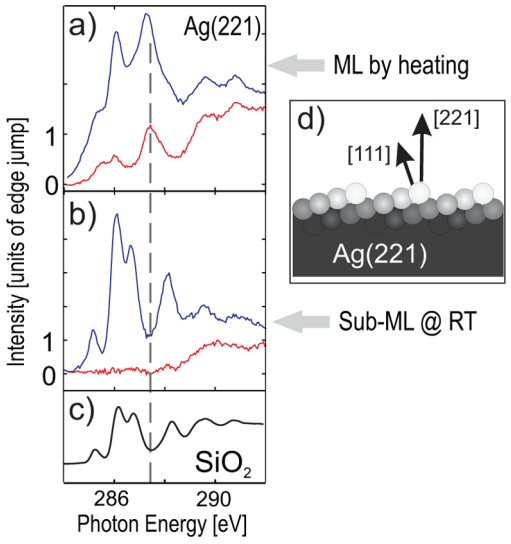

Figure 3. Effect of surface steps on the thermal decomposition of PFP on a stepped Ag(221) surface of which geometry is drawn schematically in part d. Comparison of carbon edge NEXAFS spectra obtained for PFP films on Ag(221), (a) prepared by thermal desorption of excessive multilayers at 410 K and (b) submonolayer film produced by deposition of less than 2 Å at RT. Like in Figure 2, the same color code is used to denote the angles of incidence while a NEXAFS spectrum of PFP on SiO_2 is shown for comparison in part c.

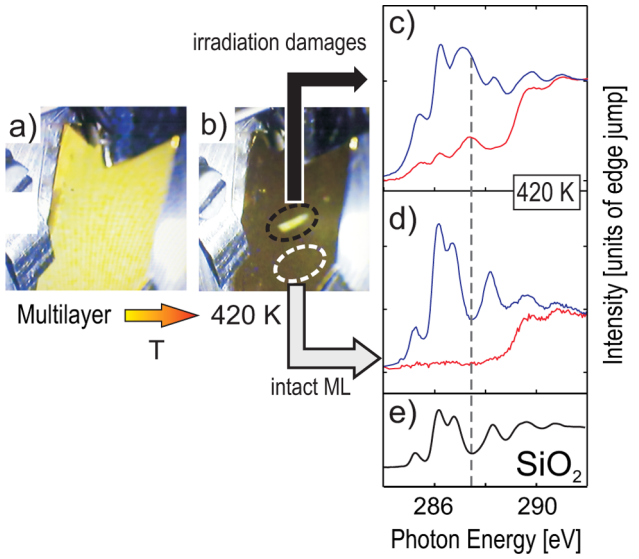

Figure 4. Radiation damage of PFP multilayers. Photographs a and b show an irradiated PFP multilayer on Au(111) before and after heating. While the intact multilayer thermally desorbs, the irradiated layer remains visible (black ellipse). NEXAFS spectra of such beam damaged areas are shown in part c and are compared to areas which had not been irradiated prior to thermal desorption in part d. Like in Figure 2, the same color code is used to denote the angles of incidence, while a NEXAFS spectrum of PFP on SiO_2 is shown for comparison in part e.

activated decomposition which is largely promoted by step edges.

Beam Damages. Though the photon flux at the used dipole beamline is moderate, possible radiation induced damages always have to be considered when analyzing changes in the NEXAFS signature of organic films.[47−50] A striking phenomenon which proves the presence of massive beam damages can be observed when comparing the thermal stability of PFP multilayers with and without former exposure to synchrotron radiation. Figure 4a depicts a photograph of a 22 nm PFP film deposited on Au(111) which appears yellowish due to diffuse scattered light from the rough multilayer film.[14] After XPS and NEXAFS measurements of this film had been carried out, the sample was heated to 420 K in order to prepare a nominal monolayer by desorbing the excessive multilayer. As shown in Figure 4b, the sample color is changed except at the position which had been illuminated by the synchrotron light (marked by the dashed black ellipse). XPS spectra that were recorded at this thoroughly illuminated region after the annealing treatment are virtually indistinguishable from measurements taken at the very beginning. However, the belonging peak intensities are distinctly larger than for a monolayer film, hence proving the presence of remaining multilayers. This finding indicates an enhanced thermal stability of the irradiated PFP film and suggests the appearance of a cross-linking process like it was found previously for aromatic SAMs.[51] On the basis of the XPS data, the stoichiometry of the irradiated films seems to be practically unaffected, thus rendering NEXAFS a much more sensitive tool, as it probes the unoccupied frontier orbitals. In fact, accompanied NEXAFS data that were recorded at this position after the annealing treatment again show the appearance of the additional resonance at about 287.3 eV (see Figure 4c) similar to the case of PFP monolayer films on Cu(111) and on Ag(221). Interestingly, the positions of the monolayer film that have not been illuminated before by synchrotron light do not show this new NEXAFS resonance and instead exhibit an undisturbed NEXAFS spectrum, as depicted in Figure 4d. We note further that this spectrum also does not change even when illuminating this spot for more than 30 min, which indicates an enhanced radiation stability of the monolayer compared to PFP multilayers. Additional experiments that were carried out by irradiating multilayer films with synchrotron light with energies of 300 and 720 eV revealed no noticeable difference. This finding suggests that the occurring damages are not due to resonant excitations or a direct photon induced process within the molecule but rather can be attributed to secondary electrons excited in the metal substrate underneath.

Total-Energy Calculations. A number of plausible starting configurations were probed in order to determine the adsorption geometry of single PFP molecules on the (111) surface of Cu, Ag, and Au. Irrespective of the substrate, PFP is found to only weakly interact with the metal surface. The calculated charge densities do not indicate the formation of covalent bonds or any significant charge transfer between substrate and adsorbate. Rather, the molecules adsorb with a relatively large distance of 3.49, 3.53, and 3.65 Å above the (111) surface of Cu, Ag, and Au. We calculate adsorption energies ΔE_{ads} of −2.84, −1.74, and −1.56 eV for the three substrates corresponding to the reaction

$$PFP_g + M \rightleftharpoons PFP@M \quad \Delta E_{ads}$$

Previous DFT-D calculations by Toyoda et al.[11] resulted in respective equilibrium distances of 2.9, 3.2, and 3.2 Å and adsorption energies of −2.17, −2.40, and −2.68 eV for Cu, Ag, and Au. The difference in the present results may partially be related to numerical differences such as the smaller number of layers used to model the substrate in ref 11, Additionally, according to observations of Reuter's group,[28] the Grimme scheme[52] used by Toyoda et al. results in stronger and shorter

dx.doi.org/10.1021/jp307316r | J. Phys. Chem. C XXXX, XXX, XXX−XXX

adsorbate−substrate bonds than the DFT-D implementation used in the present work.

Next, we consider the partial dissociation of PFP. Since for nonfluorinated acenes the largest reactivity is found for the central ring,[53,54] we model the case that a single fluorine atom dissociates from the central ring of either the surface adsorbed or gas-phase PFP molecule according to

$$\mathrm{PFP@M} \rightleftharpoons \mathrm{C_{22}F_{13}@M} + \mathrm{F^{\bullet}_g} \quad \Delta E_{\mathrm{diss}}$$

$$\mathrm{PFP_g} \rightleftharpoons \mathrm{C_{22}F^{\bullet}_{13g}} + \mathrm{F^{\bullet}_g} \quad \Delta E_{\mathrm{diss}}(\mathrm{gas})$$

The calculated energies ΔE_{diss} are summarized in Table 1. The corresponding value for the gas phase is $\Delta E_{\mathrm{diss}}(\mathrm{gas})$ = 5.4 eV.

Table 1. Adsorption and Dissociation Energies Calculated within DFT-D as Defined in the Text

E (eV)	Cu(111)	Ag(111)	Au(111)
ΔE_{ads}	−2.8	−1.7	−1.6
ΔE_{diss}	3.3	3.8	4.1
$\Delta E_{\mathrm{diss}}(\mathrm{gas}) - E_{\mathrm{diss}}$	2.1	1.6	1.3
$\Delta E^{\bullet}_{\mathrm{ads}}$	−4.0	−2.7	−2.5
$\Delta E^{\bullet}_{\mathrm{ads}} - \Delta E_{\mathrm{ads}}$	−1.2	−1.0	−0.9
$\Delta E_{\mathrm{diss}}(\mathrm{surf})$	−1.9	−0.1	0.4

Obviously, the dissociation of surface adsorbed PFP requires considerably less energy than the corresponding reaction in the gas phase, in particular for Cu and Ag substrates. This is surprising, given the rather weak interaction between PFP and substrate. In order to better understand this phenomenon, we calculated the adsorption energy of the partially defluorinated PFP according to

$$\mathrm{C_{22}F^{\bullet}_{13g}} + \mathrm{M} \rightleftharpoons \mathrm{C_{22}F_{13}@M} \quad \Delta E^{\bullet}_{\mathrm{ads}}$$

Obviously, the energy released upon adsorption of the partially defluorinated PFP, $\Delta E^{\bullet}_{\mathrm{ads}}$, is of the order of 1 eV larger than ΔE_{ads} (see Table 1). This increase in adsorption energy is accompanied by a change in adsorption characteristics. As shown in Figure 5, upon F dissociation, the formerly weakly physisorbed PFP forms a strong C−M bond, which is accompanied by a considerable distortion of the molecular adsorption geometry, leading to a bending of the aromatic backbone. This is consistent with our NEXAFS findings, which showed a notable change in dichroism. If one compares the energy difference $\Delta E^{\bullet}_{\mathrm{ads}} - \Delta E_{\mathrm{ads}}$ with the substrate-induced change in the dissociation energy ΔE_{diss}, one finds the same trend: The less noble the substrate, the stronger the increase in adsorption energy and the stronger the decrease in dissociation energy. The above results show that the possibility of broken-bond healing provided by the coinage-metal substrate is largely responsible for the catalytic action observed experimentally. We mention that a similar effect has recently been found to catalyze the polymerization of tetraazaperopyrene on Cu(111).[55]

While the calculations so far allow for understanding the chemical trend, they certainly do not model the majority of dissociation events. It can be expected that the F dissociation followed by lateral diffusion has a lower activation energy than the immediate F desorption into the gas phase. In order to elucidate the initial stages of this process, we consider the reaction

$$\mathrm{PFP@M} \rightleftharpoons \mathrm{C_{22}F_{13}@M} + \mathrm{F@M} \quad \Delta E_{\mathrm{diss}}(\mathrm{surf})$$

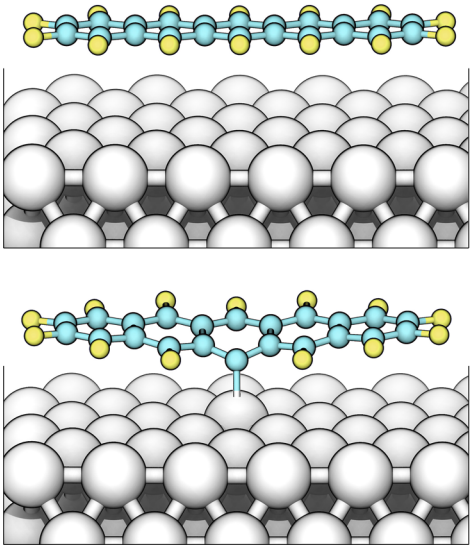

Figure 5. Calculated geometry of intact (top, $C_{22}F_{14}$) and partly defluorinated (bottom, $C_{22}F_{13}$) PFP adsorbed on the Ag(111) surface.

for the case of the Ag(111) surface. In Figure 6, we show the calculated energy landscape $\Delta E_{\mathrm{diss}}(\mathrm{surf})$ seen by a dissociated fluorine atom moving laterally away from the PFP molecule. The potential energy surface has been calculated by fixing the lateral position of the dissociated F atom as well as the two carbon positions farthest away from this fluorine, while all remaining degrees of freedom were allowed to relax. As expected, we find the energy barrier for dissociating the F laterally considerably smaller than that for a vertical reaction path; it amounts to 2.1 eV. Once this barrier is overcome, the originally PFP dissociated F atom adsorbs most favorably in 3-fold coordinated bridge position. Finally, an energy gain of 0.1 eV is realized for dissociation on the Ag(111) surface. It is considerably larger on Cu (1.9 eV, cf. Table 1), whereas energy is required (0.4 eV, cf. Table 1) to dissociate PFP on Au. This explains why the majority of PFP molecules on gold will desorb intactly upon heating, in contrast to Ag and Cu, where dissociation is thermodynamically more favored.

Once partially dissociated PFP molecules are covalently bond to the Cu or Ag substrate, additional cleavage of fluorine will occur, eventually leading to an almost complete defluorination. Regarding the separated fluorine atoms, several reaction paths are conceivable. Comparing the corresponding standard enthalpy of formation of the various metal fluorides ($\Delta_f H^0_s$(CuF) = −2.91 eV,[56] $\Delta_f H^0_s$(AgF) = −2.12 eV,[57] AuF not stable) indicates that they can be formed only on silver or copper. Alternatively, the desorbing F radical can further react with hydrogen (i.e., from covered walls of the vacuum vessel), leading to the formation of the stable HF ($\Delta_f H^0_g$(HF) = −2.83 eV[56]) which could be detected in previous thermal desorption spectra of PFP films adsorbed on Ag(111).[14] The fact that metal fluoride species were only observed in our XPS data for copper but not for silver (cf. Figure 1e) is consistent with these values because only CuF is more stable than the most likely path of fluorine desorption upon heating.

DISCUSSION

The present measurements show distinct differences in the chemical stability of PFP films on the various coinage metal surfaces. Though PFP is only weakly adsorbed on Au(111), this

dx.doi.org/10.1021/jp307316r | J. Phys. Chem. C XXXX, XXX, XXX−XXX

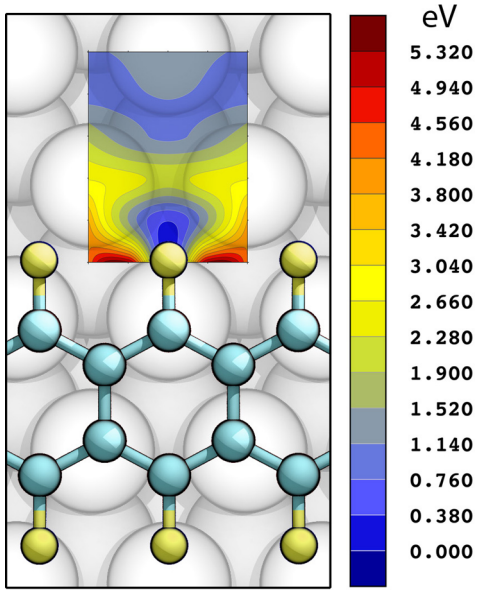

Figure 6. Calculated potential energy surface of the lateral F dissociation from PFP on Ag(111); see text.

interaction exceeds the intermolecular cohesion and allows for a controlled thermal desorption of multilayers. The remaining nominal monolayer reveals neither any broadening of the π^* resonances in the C1s NEXAFS spectra as compared to the bulk data nor a change in the stoichiometry upon heating to temperatures of more than 500 K. Only a continuous decrease of the PFP related intensity occurs for temperatures above 450 K which is indicative for desorption of intact molecules. This physisorption of PFP on Au(111) and Ag(111) at room temperature is in pronounced difference to the adsorption of the nonfluorinated pentacene, where a substantial broadening of the π^* resonances was found for monolayer films on both substrates.[15,58] By contrast, on Cu(111), a significant defluorination takes place already during thermal desorption of multilayer films at about 430 K, which is accompanied by a reduced dichroism of the carbon edge NEXAFS signatures. A temperature induced surface reaction of PFP films on Cu(111) has also been reported previously by Glowatzki et al.[12] In that study, it was further found that after extensive heating of submonolayer films (135 min at 425 K) the adsorbed molecules were fixated so that they could be imaged by means of scanning tunneling microscopy at room temperature while nonheated films appear to be quite mobile. The presently identified decomposition of PFP on Cu(111) continues upon further heating until the layer is almost completely defluorinated at 600 K, leaving a fluorine-free carbon film behind. For comparison, a monolayer of the nonfluorinated pentacene adsorbed on Cu(110) can sustain heating to these temperatures without any degradation.[13] Interestingly, a noticeable degradation was also observed for PFP films on Ag(111) when heating above 440 K. As one would expect, this indicates that the reactivity of silver is in between that of Au and Cu, being strongest for copper. The appearance of a temperature-induced decomposition of PFP molecules on Ag(111) in spite of their physisorption at room temperature indicates a metastable equilibrium of the intact layer. This observation is at variance with the findings of a previous DFT-based analysis of PFP monolayers adsorbed on the (111)-oriented surfaces of these three coinage metals,[11] where the largest adsorption energy was found for gold and the smallest one for copper. On the contrary, the trend found in the experimental data is well reproduced by the DFT-D calculations of the present study. By also considering chemical recations at the molecule−metal interface, it was possible to unravel the observed defluorination mechanism in our theoretical analysis. Though fluorine separation is a thermally activated process, the system benefits from an overall energy gain upon covalent C−M bonding of partially dissociated PFP molecules to the metal surface as well as the formation of metal fluorides in the case of Cu and Ag substrates. Interestingly, in contrast to CuF, no AgF related signal could be detected in the XPS data which suggests that fluorine is only weakly bound at the Ag(111) surface and may thermally desorb at temperatures where PFP becomes defluorinated. Additional measurements on PFP adsorbed on the stepped Ag(221) surface showed a reduced barrier for defluorination which occurs already at lower temperatures, thus demonstrating the catalytic effect of steps. The latter result is of particular relevance for device applications, since electrodes in electronic devices are polycrystalline and exhibit numerous defects so that defluorination is expected to occur already at lower temperatures slightly above room temperature. In this respect, the barriers of decomposition obtained from theoretical analysis of the interaction of PFP with ideal, defect-free (111) surfaces should only be considered as an upper limit, whereas real surfaces always exhibit defects which lower this barrier.

CONCLUSIONS

Large differences in the thermal and chemical stability of PFP thin films adsorbed on the coinage metal surfaces of Cu, Ag, and Au were observed. Only on gold PFP desorbs without any noticeable decomposition, while Ag and Cu catalyze a partial defluorination, leading to a distortion of the adsorption geometry. Our DFT-D calculations showed that, even on the noble metal silver, defluorination and subsequent covalent binding of PFP to the metal are energetically favored against desorption. The present study indicates that fluorinated aromatic hydrocarbons, though exhibiting interesting electronic properties such as n-type conduction and robustness against oxidation, might actually be less stable in contact with metal surfaces than their nonfluorinated analogues. It thus emphasizes the importance of not only characterizing possible energy level alignment with respect to the Fermi level of metal substrates but also analyzing the chemical stability to validate their use for organic electronic device applications.

AUTHOR INFORMATION

Corresponding Author

*E-mail: gregor.witte@physik.uni-marburg.de.

Notes

The authors declare no competing financial interest.

ACKNOWLEDGMENTS

We acknowledge the Helmholtz-Zentrum Berlin - Electron storage ring BESSY II for provision of synchrotron radiation at beamline HE-SGM and travel support as well as the HLRS Stuttgart and the Paderborn PC^2 for providing supercomputer time. We gratefully acknowledge financial support by the Friedrich-Ebert-Stiftung (T.B.) as well as by the Deutsche Forschungsgemeinschaft (S.W. and W.G.S.).

REFERENCES

(1) Anthony, J. E.; Facchetti, A.; Heeney, M.; Marder, S. R.; Zhan, X. W. *Adv. Mater.* **2010**, *22*, 3876−3892.
(2) Jung, B. J.; Tremblay, N. J.; Yeh, M. L.; Katz, H. E. *Chem. Mater.* **2011**, *23*, 568−582.
(3) Kagan, C. R.; Afzali, A.; Graham, T. O. *Appl. Phys. Lett.* **2005**, *86*, 193505.
(4) Sirringhaus, H. *Adv. Mater.* **2009**, *21*, 3859−3873.
(5) Angelis, F. D.; Gaspari, M.; Procopio, A.; Cuda, G.; Fabrizio, E. D. *Chem. Phys. Lett.* **2009**, *468*, 193−196.
(6) Delgado, M. C. R.; Pigg, K. R.; Filho, D. A. d. S.; Gruhn, N. E.; Sakamoto, Y.; Suzuki, T.; Malave Osuna, R.; Casado, J.; Hernandez, V.; Lopez Navarrete, J. T.; Martinelli, N. G.; Cornil, J.; Sanchez-Carrera, R. S.; Coropceanu, V.; Bredas, J.-L. *J. Am. Chem. Soc.* **2009**, *131*, 1502−1512.
(7) Sakamoto, Y.; Suzuki, T.; Kobayashi, M.; Gao, Y.; Fukai, Y.; Inoue, Y.; Sato, F.; Tokito, S. *J. Am. Chem. Soc.* **2004**, *126*, 8138.
(8) Koch, N.; Vollmer, A.; Duhm, S.; Sakamoto, Y.; Suzuki, T. *Adv. Mater.* **2007**, *19*, 112.
(9) Koch, N.; Gerlach, A.; Duhm, S.; Glowatzki, H.; Heimel, G.; Vollmer, A.; Sakamoto, Y.; Suzuki, T.; Zegenhagen, J.; Rabe, J. P.; Schreiber, F. *J. Am. Chem. Soc.* **2008**, *130*, 7300.
(10) Duhm, S.; Hosoumi, S.; Salzmann, I.; Gerlach, A.; Oehzelt, M.; Wedl, B.; Lee, T.-L.; Schreiber, F.; Koch, N.; Ueno, N.; Kera, S. *Phys. Rev. B* **2010**, 81.
(11) Toyoda, K.; Hamada, I.; Lee, K.; Yanagisawa, S.; Morikawa, Y. *J. Phys. Chem. C* **2011**, *115*, 5767−5772.
(12) Glowatzki, H.; Heimel, G.; Vollmer, A.; Wong, S. L.; Huang, H.; Chen, W.; Wee, A. T. S.; Rabe, J. P.; Koch, N. *J. Phys. Chem. C* **2012**, *116*, 7726−7734.
(13) Söhnchen, S.; Lukas, S.; Witte, G. *J. Chem. Phys.* **2004**, *121*, 525−534.
(14) Götzen, J.; Schwalb, C. H.; Schmidt, C.; Mette, G.; Marks, M.; Höfer, U.; Witte, G. *Langmuir* **2011**, *27*, 993−999.
(15) Käfer, D.; Witte, G. *Chem. Phys. Lett.* **2007**, *442*, 376−383.
(16) Dilella, D.; Smardzewski, R.; Guha, S.; Lund, P. *Surf. Sci.* **1985**, *158*, 295−306.
(17) Vijayalakshmi, S.; Fohlisch, A.; Kirchmann, P. S.; Hennies, F.; Pietzsch, A.; Nagasono, M.; Wurth, W. *Surf. Sci.* **2006**, *600*, 4972−4977.
(18) National Institute of Standards and Technology, *NIST X-ray Photoelectron Spectroscopy Database* 2003.
(19) Shirley, D. A. *Phys. Rev. B* **1972**, *5*, 4709−4714.
(20) Stöhr, J. In *NEXAFS Spectroscopy*; Gomer, R., Ed.; Springer: Berlin, Germany, 1992.
(21) Marks, M.; Schmidt, C.; Schwalb, C. H.; Breuer, T.; Witte, G.; Höfer, U. *J. Phys. Chem. C* **2012**, *116*, 1904−1911.
(22) Kresse, G.; Furthmüller, J. *Comput. Mater. Sci.* **1996**, *6*, 15.
(23) Perdew, J. P.; Chevary, J. A.; Vosko, S. H.; Jackson, K. A.; Pederson, M. R.; Singh, D. J.; Fiolhais, C. *Phys. Rev. B* **1992**, *46*, 6671.
(24) Kresse, G.; Joubert, D. *Phys. Rev. B* **1999**, *59*, 1758.
(25) Schmidt, W. G.; Seino, K.; Preuss, M.; Hermann, A.; Ortmann, F.; Bechstedt, F. *Appl. Phys. A: Mater. Sci. Process.* **2006**, *85*, 387.
(26) Rohlfing, M.; Bredow, T. *Phys. Rev. Lett.* **2008**, *101*, 266106.
(27) Atodiresei, N.; Caciuc, V.; Lazić, P.; Blügel, S. *Phys. Rev. Lett.* **2009**, *102*, 136809.
(28) Mcnellis, E. R.; Meyer, J.; Reuter, K. *Phys. Rev. B* **2009**, *80*, 205414.
(29) Mercurio, G.; McNellis, E. R.; Martin, I.; Hagen, S.; Leyssner, F.; Soubatch, S.; Meyer, J.; Wolf, M.; Tegeder, P.; Tautz, F. S.; Reuter, K. *Phys. Rev. Lett.* **2010**, *104*, 036102.
(30) Thierfelder, C.; Witte, M.; Blankenburg, S.; Rauls, E.; Schmidt, W. G. *Surf. Sci.* **2011**, *605*, 746.
(31) Ortmann, F.; Schmidt, W. G.; Bechstedt, F. *Phys. Rev. Lett.* **2005**, *95*, 186101.
(32) Ortmann, F.; Bechstedt, F.; Schmidt, W. G. *Phys. Rev. B* **2006**, *73*, 205101.
(33) Dion, M.; Rydberg, H.; Schröder, E.; Langreth, D. C.; Lundqvist, B. I. *Phys. Rev. Lett.* **2004**, *92*, 246401.
(34) Lazić, P.; Atodiresei, N.; Alaei, M.; Caciuc, V.; Blügel, S.; Brako, R. *Comput. Phys. Commun.* **2010**, *181*, 371.
(35) de Oteyza, D. G.; Wakayama, Y.; Liu, X.; Yang, W.; Cook, P. L.; Himpsel, F. J.; Ortega, J. E. *Chem. Phys. Lett.* **2010**, *490*, 54−57.
(36) Hinderhofer, A.; Heinemeyer, U.; Gerlach, A.; Kowarik, S.; Jacobs, R. M. J.; Sakamoto, Y.; Suzuki, T.; Schreiber, F. *J. Chem. Phys.* **2007**, *127*, 194705.
(37) Breuer, T.; Witte, G. *Phys. Rev. B* **2011**, *83*, 155428.
(38) Rocco, M. L. M.; Haeming, M.; Batchelor, D. R.; Fink, R.; Schöll, A.; Umbach, E. *J. Chem. Phys.* **2008**, *129*, 074702.
(39) Note, that this small final state effect differs from the larger core-hole screening effect found in XPS (0.7−1.15 eV).[35]
(40) Mainka, C.; Bagus, P. S.; Schertel, A.; Strunskus, T.; Grunze, M.; Wöll, C. *Surf. Sci.* **1995**, *341*, L1055−L1060.
(41) Weiss, K.; Gebert, S.; Wuhn, M.; Wadepohl, H.; Wöll, C. *J. Vac. Sci. Technol., A* **1998**, *16*, 1017−1022.
(42) Liu, A. C.; Stöhr, J.; Friend, C. M.; Madix, R. J. *Surf. Sci.* **1990**, *235*, 107−115.
(43) Chen, Q.; McDowall, A.; Richardson, N. *Langmuir* **2003**, *19*, 10164−10171.
(44) Blakely, D. W.; Somorjai, G. A. *J. Catal.* **1976**, *42*, 181−196.
(45) Götzen, J.; Lukas, S.; Birkner, A.; Witte, G. *Surf. Sci.* **2011**, *605*, 577−581.
(46) The silver (221) surface consists of (111) terraces with an inclination of 15.8° with respect to the macroscopic (221) surface plane. Therefore, molecules which lie flat on the (111) terraces are expected to exhibit a molecular orientation of 15.8° relative to the (221) surface determined by NEXAFS.
(47) Zharnikov, M.; Grunze, M. *J. Vac. Sci. Technol., B* **2002**, *20*, 1793−1807.
(48) Zubavichus, Y.; Zharnikov, M.; Shaporenko, A.; Fuchs, O.; Weinhardt, L.; Heske, C.; Umbach, E.; Denlinger, J. D.; Grunze, M. *J. Phys. Chem. A* **2004**, *108*, 4557−4565.
(49) Feulner, P.; Niedermayer, T.; Eberle, K.; Schneider, R.; Menzel, D.; Baumer, A.; Schmich, E.; Shaporenko, A.; Tai, Y.; Zharnikov, M. *Phys. Rev. Lett.* **2004**, *93*, 178302.
(50) Zubavichus, Y.; Fuchs, O.; Weinhardt, L.; Heske, C.; Umbach, E.; Denlinger, J. D.; Grunze, M. *Radiat. Res.* **2004**, *161*, 346−358.
(51) Turchanin, A.; Käfer, D.; El-Desawy, M.; Wöll, C.; Witte, G.; Gölzhauser, A. *Langmuir* **2009**, *25*, 7342−7352.
(52) Grimme, S. *J. Comput. Chem.* **2006**, *27*, 1787.
(53) Zander, M. *Polycyclic Hydrocarbons*; Academic Press: London, UK, 1964.
(54) Schleyer, P. V.; Manoharan, M.; Jiao, H. J.; Stahl, F. *Org. Lett.* **2001**, *3*, 3643−3646.
(55) Blankenburg, S.; Rauls, E.; Schmidt, W. G. *J. Phys. Chem. Lett.* **2010**, *1*, 3266.
(56) Chase, M. *NIST-JANAF Thermochemical Tables 2 Volume-Set (Journal of Physical and Chemical Reference Data Monographs)*; American Institute of Physics: Woodbury, N.Y., USA, 1998.
(57) Lide, D. R., Ed. *CRC Handbook of Chemistry and Physics*, 89th ed.; CRC Press: Boca Raton, FL, USA, 2008−2009.
(58) Käfer, D.; Ruppel, L.; Witte, G. *Phys. Rev. B* **2007**, *75*, 085309.